Shear-Induced Instability of Sand Containing Fines: Using the Equivalent Intergranular Void Ratio as a State Variable

Ehsan Yazdani, S.M.ASCE[1]; Amy Nguyen[2]; and T. Matthew Evans, M.ASCE[3]

Abstract: In this work, the influence of different types of fine materials on the shear-induced instability of sand–fines mixtures was studied from various aspects. For this purpose, clean sand was mixed with three kinds of fines with different plasticity indices (PIs)—silt ($PI=15$), clay ($PI=21$), and diatomaceous silt ($PI=70$). A new fines classification system was used that suggested that the high PI of diatomaceous silt is not due to electrochemical forces, but to the porous skeletons of diatoms producing high Atterberg limits. Multiple series of undrained triaxial tests were performed in order to evaluate the collapsibility potential of the mixtures. The equivalent intergranular void ratio, as a state variable, was used to evaluate the behavior of the mixtures. It was found that the equivalent intergranular void ratio can reduce the influence of fines and provide a strong correlation bearing several aspects of the mechanical behavior of coarse-grained–fines mixtures.
DOI: 10.1061/(ASCE)GM.1943-5622.0002486.

Introduction

During earthquakes, a wide range of shear strains are applied to the soil, causing the generation of pore water pressure in loose to medium-consistency sandy soils, often followed by a critical reduction in effective stress that is influenced by the soil's physical and index properties (Altun et al. 2005; Belkhatir et al. 2011). Therefore, geotechnical engineers are interested in assessing the effects of various types of fines on the liquefaction potential of sand–fines mixtures. There are multiple factors that can affect the role of fines in the behavior of sand–fines mixtures, such as the plasticity index (PI), fines content, degree of cementation, overconsolidation ratio, soil fabric, and stress history (Shen et al. 1977; Ishihara et al. 1978; Bouferra and Shahrour 2004; Park and Kim 2013). Significant efforts have been expended in explaining the effect of fines on soil liquefaction, but contradictory conclusions have been reported in the literature. Some studies have found that liquefaction resistance increases with the addition of silty fines (Ishihara et al. 1978; Okusa et al. 1980; Garga and McKay 1984; Bolton Seed et al. 1985; Vaid 1994; Amini and Qi 2000), whereas others have demonstrated a reduction in liquefaction resistance (Shen et al. 1977; Ishihara et al. 1980; Throncoso and Verdugo 1985; Yasuda et al. 1994; Chien et al. 2002). Several more-recent studies have reported an increase in liquefaction susceptibility up to a certain fines content, followed by a decreasing response (Thevanayagam 2000; Polito and Martin 2001; Xenaki and Athanasopoulos 2003; Bouckovalas et al. 2003; Naeini and Baziar 2004; Hazirbaba and Rathje 2009; Porcino and Diano 2017; Koester 2018; Rahman and Sitharam 2020).

There is no universally agreed-upon explanation of the role of plasticity in the evaluation of liquefaction susceptibility. Perlea (2000) noted that, despite shear-induced excess pore water pressure, "cohesion" prevents particles from separating, and therefore the loss of strength is generally greater in loose granular soils, although structural collapse and runaway deformation, as a result of the rearrangement of particles, usually happens under both undrained and drained conditions. Guo and Prakash (1999) demonstrated that the cohesive character of fines with high PI values serves to enhance their resistance to liquefaction. Park and Kim (2013) explored the effect of the plasticity of fines on the liquefaction resistance of sandy soils with different density states. The results indicated that the effect of plasticity on liquefaction resistance was more pronounced in denser-packed sands than looser assemblies (Gobbi et al. 2022); as the plasticity of the fines increased, denser specimens exhibited a significant reduction in liquefaction resistance. Bouferra and Shahrour (2004) emphasized that even small amounts of clay fines increase liquefaction susceptibility by prohibiting the specimen from dilating—that is, plastic fines reduce the dilatant tendency of sand matrices.

In this study, three different types of fine-grained soils were used to explore the role of plasticity on the instability of sand–fines mixtures. Clay, silt, and diatomaceous silt (DS) were used to provide insights into the effects of the percentage of fines and their PI on the various aspects of collapse potential. To provide a tangible comparison, the shear-induced instability of mixtures under undrained conditions was quantified. One reason for the contradictory reports in the literature concerning the effects of fines on liquefaction susceptibility is the different density variables used in interpreting the results. In this work, the equivalent intergranular void ratio was used in order to provide more useful insights into the mechanical response of sand–fines mixtures. Previous experimental studies have focused mainly on concepts from critical-state soil mechanics (i.e., the behavior in the $e - \log p'_{cr}$ plane) for verifying active fines-fraction approximations. In this study, in addition to considering the volumetric response, the authors strived to employ a different framework in order to examine the active fines fraction not only in the critical state, but also in different stages of shearing, such as at the peak and phase-transformation points. The instability and collapsibility framework presented

[1]Yamamuro Fellow and Graduate Research Assistant, School of Civil and Construction Engineering, Oregon State Univ., Corvallis, OR 97331. ORCID: https://orcid.org/0000-0003-0027-0820

[2]Staff Engineer, Geoengineers, Seattle, WA; Formerly, Graduate Research Assistant, School of Civil and Construction Engineering, Oregon State Univ., Corvallis, OR 97331.

[3]Professor, School of Civil and Construction Engineering, Oregon State Univ., Corvallis, OR 97331 (corresponding author). ORCID: https://orcid.org/0000-0002-8457-7602. Email: matt.evans@oregonstate.edu

Note. This manuscript was submitted on September 17, 2021; approved on March 29, 2022; published online on June 1, 2022. Discussion period open until November 1, 2022; separate discussions must be submitted for individual papers. This paper is part of the ***International Journal of Geomechanics***, © ASCE, ISSN 1532-3641.

includes a variety of indices that are able to capture the onset of liquefaction, the collapse potential, dilation tendency, and degree of collapsibility when coarse-grained–fines mixtures are sheared.

Diatomaceous Soils and Other Tested Materials

Diatoms are single-celled microorganisms found in marine and freshwater environments. They are generally observed to have two different shapes: radial or bilaterally symmetrical. Diatoms are surrounded by a hard and porous silica cell wall called a frustule [Fig. 1(c)]. Distinct index properties of diatomaceous deposits in comparison with other sediments have been noted in the literature, with high inter- and intraparticle porosity and low specific gravity being two of the inherent features of diatomaceous deposits (Sonyok 2015; Caicedo et al. 2018; Evans and Moug 2020; Wang et al. 2021; Yazdani et al. 2021). It has generally been hypothesized that the unusually high PI values of diatomaceous material are likely due to water being held in large volumes in intraparticle pores, and not due to its mineralogy. High friction angles and high plasticity are typical of diatomaceous soils. This combination is inconsistent with observations on the behavior of more "textbook" soils, in which increasing plasticity is typically associated with a reduction in friction angle, while diatomaceous deposits exhibit a reversed behavior.

Four baseline soils were used in this study for the purposes of assessing the effects of the mineralogy, plasticity, and gradation of different fines on the behavior of coarse-grained–fines mixtures. The host material was a uniformly graded fine sand obtained as grab samples of Agate Beach sand (BS) taken from near Newport, Oregon. The samples were washed over a No. 200 sieve to ensure only the coarse-grained particles were retained. Three fine-grained soils were used, colloquially referred to as Willamette Silt (WS), Umpqua Clay (UC), and DS. The WS was obtained, using Shelby tubes and split-spoon sampling, from Corvallis, Oregon, the UC as grab samples from Reedsport, Oregon, and the DS as split-spoon

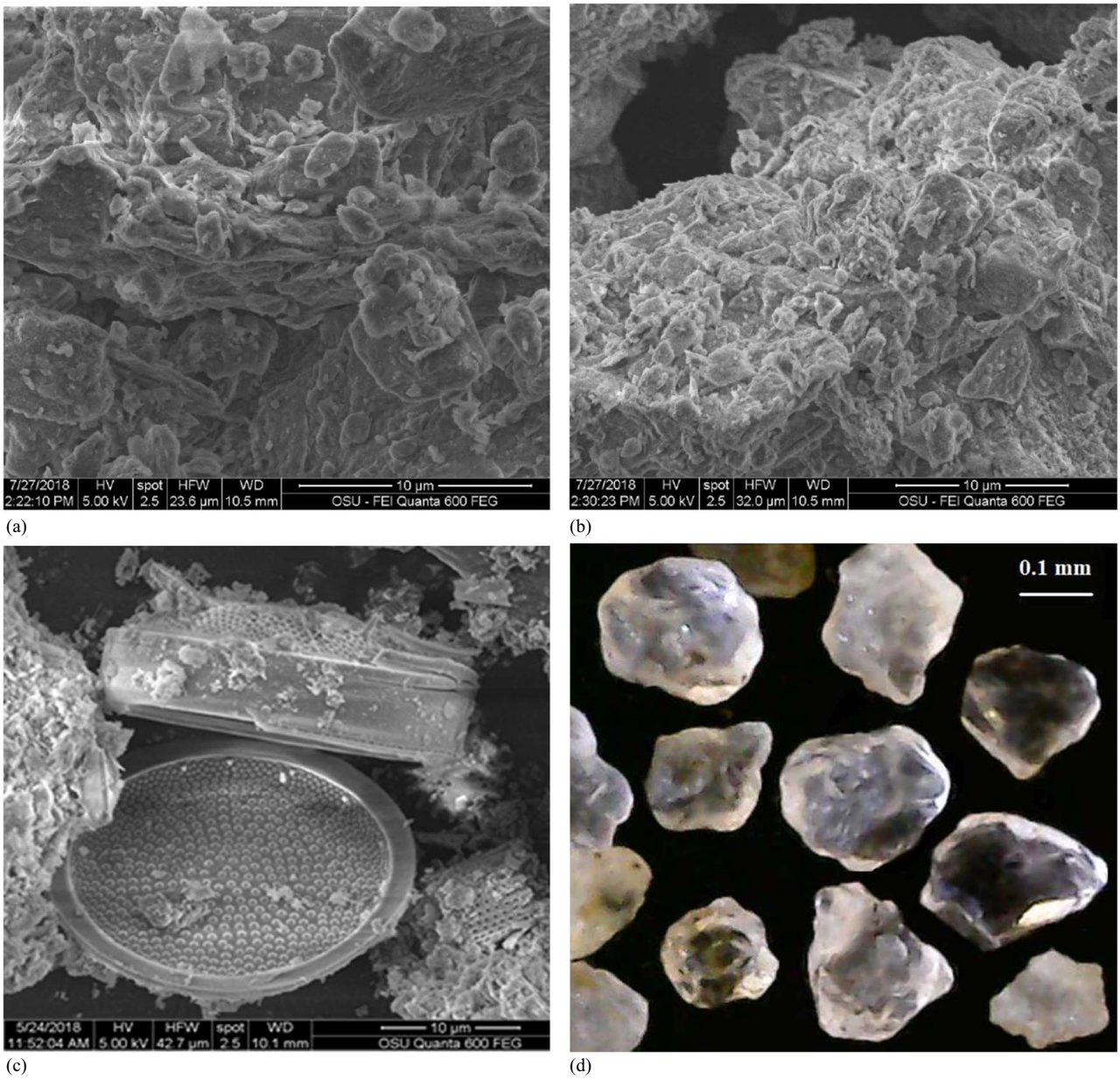

Fig. 1. SEM images of the baseline tested material: (a) WS; (b) UC; (c) DS; and (d) Agate BS.

Int. J. Geomech., 2022, 22(8): 04022121

samples from close to Buck Creek in Umatilla National Forrest, Oregon. Scanning electron microscope (SEM) photomicrographs of the four materials are presented in Fig. 1.

Material Characterization

Index Properties

The physical properties of the tested materials are provided in Table 1. The soil mixtures were prepared using different types of fines in mass percentages of 10%, 20%, and 30%.

Grain-size distribution curves for the baseline materials were measured according to ASTM D6916 (ASTM 2004) and ASTM D7928 (ASTM 2016). The results are presented in Fig. 2. The SEM images provide a precise look into the shapes of the components of the materials. The DS primarily comprised rigid silica diatom frustules (exoskeletons), consequently having a dramatically different particle shape to the WS and UC. The BS was generally subangular to subrounded.

Classification Based on Sensitivity to Pore-Fluid Chemistry

The engineering properties of diatomaceous soils are complex and, in many ways, not well understood. Some of their characteristics are inconsistent, from a classical soil mechanics perspective. For example, they typically possess both high plasticity and a high friction angle, which is uncommon (Mitchell and Soga 2005; Caicedo et al. 2018). In order to provide insights into the possible reasons for the high PI values of DSs, despite them containing a relatively small clay-sized fraction, we considered two different fines classification systems: Casagrande's plasticity chart, which is used in the Unified Soil Classification System (USCS) and a new chart, which exploits differing pore-fluid chemistries, presented by Jang and Santamarina (2016). In order to decrease experimental variability from the Casagrande method cup procedure and avoid the inherent uncertainty of the thread method for measuring the plastic limit of fine soil, the fall cone test was used instead (Hansbo 1957; Casagrande 1958; Sowers et al. 1960; Sherwood and Ryley 1970; Wroth and Wood 1978; Evans and Simpson 2015; Khoubani and Evans 2017).

In the fall cone test, the liquid limit is the water content of the soil when the cone penetration equals 20 mm in 5 s, which corresponds to an undrained shear strength of 1.7–2.3 kPa (Skemption and Northey 1952; Hansbo 1957; Russell and Mickle 1970; Wroth and Wood 1978; Feng 2001; Koumoto and Houlsby 2001; Mitchell and Soga 2005). Based on Skemption and Northey (1952), the undrained shear strength at the plastic limit is about 100 times that at the liquid limit. Thus, it can be concluded from the theoretical concept of the fall cone test that the cone penetration at the plastic limit is 2 mm. Feng (2000) presented a linear log d–log w model for calculation of the plastic limit

$$\log w = \log c + m \log d \tag{1}$$

where w = water content; c = water content at d = 1 mm; m = slope of the flow curve; and d = depth of the cone penetration after 5 s.

To classify the fines based on the chart presented by Jang and Santamarina (2016), soil pastes were prepared for the fall cone testing using deionized water, kerosene (low permittivity), and a 2-M sodium chloride (NaCl) brine (high ionic concentration), as described in Khoubani and Evans (2017). The liquid-limit ratios were calculated from Eqs. (2) and (3), and the electrical sensitivity, S_E, was determined by Eq. (4)

$$\left[\frac{LL_{DW}}{LL_{ker}}\right]_{\text{corrected}} = \frac{LL_{DW}}{LL_{ker}} G_{ker} \tag{2}$$

$$\left[\frac{LL_{DW}}{LL_{\text{brine}}}\right]_{\text{corrected}} = \frac{LL_{DW}}{LL_{\text{brine}}}(1 - c_{\text{brine}} LL_{\text{brine}}) \tag{3}$$

$$S_E = \sqrt{\left(\frac{LL_{DW}}{LL_{\text{brine}}} - 1\right)^2 + \left(\frac{LL_{ker}}{LL_{\text{brine}}} - 1\right)^2} \tag{4}$$

where LL_{DW}, LL_{ker}, and LL_{brine} = liquid limit of the soil paste prepared with deionized water, kerosene, and 2-M NaCl brine, respectively; and G_{ker} and c_{brine} = specific gravity of kerosene and concentration of the brine, respectively. Soil can be classified based on its response to different pore fluids and by using the liquid limit and electrical sensitivity, from which the mechanical behavior can be anticipated more robustly. The soils can then be classified in terms of low, intermediate, or high plasticity fines grains of low, intermediate, or high electrical sensitivity. The results from the three different tested materials are shown in Fig. 3. The low electrical sensitivity of the DS may be explained by the fact that the predominant chemical component of the soil is silica, which is largely chemically inert. Thus, the high plasticity of the DS was due to water being held in both inter- and intraparticle porosity, rather than due to electrochemical forces, which are responsible for the high plasticity in many chemically active clays (e.g., smectites).

Table 1. Index properties of the soils

Index property	*BS*	*WS*	*UC*	*DS*
G_s	2.71	2.76	2.77	2.30
D_{60} *(mm)*	0.154	—	—	—
D_{50} *(mm)*	0.148	0.011	0.004	0.007
D_{30} *(mm)*	0.136	—	—	—
D_{10} *(mm)*	0.112	—	—	—
LL	—	36	38	120
PI	—	15	21	70
Clay fraction, <0.002 μm (%)	—	18	40	24
Unified classification	SP	CL[a]	CL	MH

Note: SP, CL and MH denote the poorly graded sand, low-plasticity clay, and high-plasticity silt, respectively.

[a]While this soil plots slightly above the "A" line on the Casagrande chart, it is colloquially referred to as "Willamette Silt," and we have adopted this convention here.

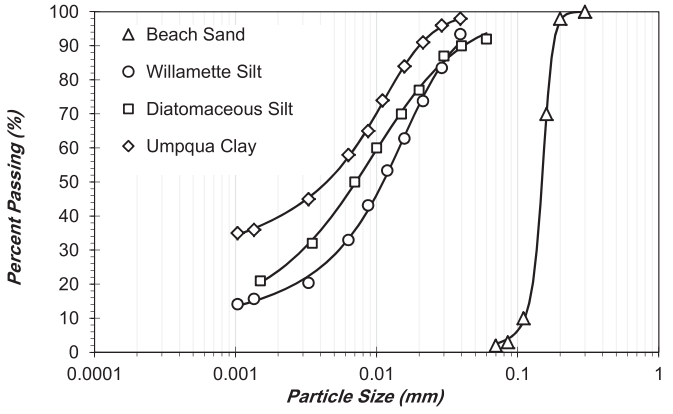

Fig. 2. Grain-size distributions of the baseline materials.

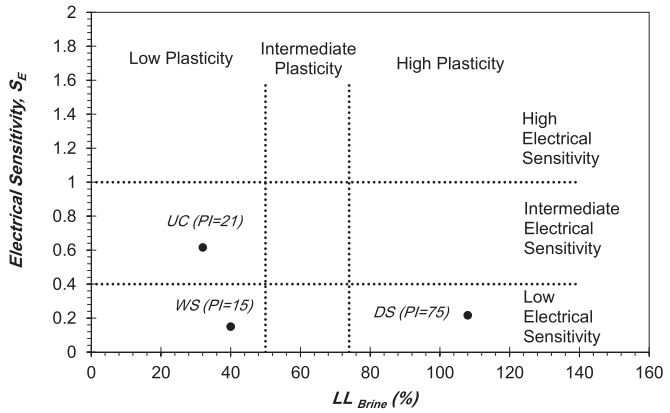

Fig. 3. Classification of fines based on electrical sensitivity and liquid limit.

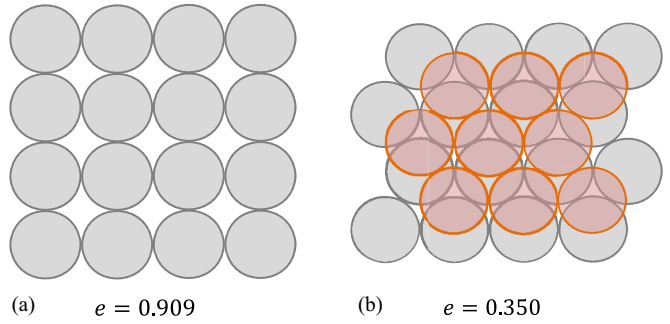

Fig. 4. Loosest and densest packing structure of monodisperse spheres: (a) simple cubic; and (b) tetrahedral.

Void Ratio in Coarse-Grained–Fines Mixtures

Threshold Fines Content and Limiting Fines Content

In order to describe the role of the fines content on the behavior of coarse-grained–fines mixtures, it was necessary to understand the stress transmission through coarse-grained–fines packing structures, and to realize how its two components interact under different density states. Percolation theory is a branch of probability theory that has effectively dealt with a wide variety of critical phenomena (Peters and Berney 2010; Herega 2015; Khoubani et al. 2020). Due to the distinct difference in particle sizes, sand–fines mixtures can be considered as binary systems. Percolation theory seeks to explain the behavior of binary packing subjected to alterations in its constituent fractions. The percolation threshold is characterized by a significant change in the response of a binary system as the result of a small change in its constituent fractions.

Monodisperse sphere packing has been extensively studied and reported on in the literature (Furnas 1928; Graton and Fraser 1935; McGeary 1961; White and Walton 1937). In the case of monodisperse spheres, five different regular packings were considered, each with a different void ratio, varying from 0.909 (simple cubic, loosest possible) to 0.350 (hexagonal, close packed, densest possible) (Fig. 4).

The variation in void ratios for other simple systems, such as bimodal mixtures of spheres, has also been investigated. When small particles drop into the primary fabric of an assembly of coarser grains, the overall volume remains constant, while the weight of the mixture increases. Thus, it can be inferred that the void ratio decreases as the amount of fines increases in a mixture. When the

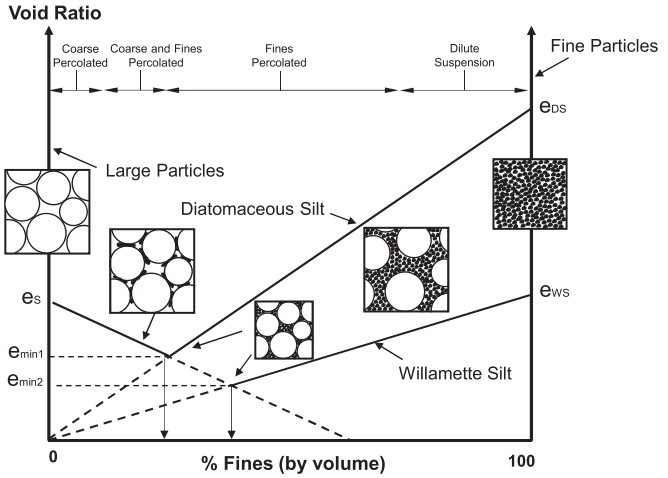

Fig. 5. Minimum void ratios for binary packing with different fines content and behavioral thresholds. (Adapted from Lade et al. 1998.)

gaps created by the coarse particles are completely filled with fines, the minimum void ratio for the binary mixture is reached, and beyond this point, by increasing the fines content, coarse grains are physically in touch with small particles, which push the larger grains apart (Lade et al. 1998). The variation in void ratio with percentage of fines for two of the tested soils is shown schematically in Fig. 5.

Simpson and Evans (2016) used percolation theory and studied behavioral thresholds in mixtures of sand and kaolinite clay, observing four behavioral regimes: (1) coarse percolated; (2) coarse and fines percolated; (3) fines percolated; and (4) dilute suspension. Interaction between coarse and fine particles leads to different degrees of consistency and compressibility in mixtures, resulting in different behavioral regimes. In the first regime, there is a continuous matrix of large particles only, leading to higher critical-state strength parameters. In the second regime, fine grains come to rest in the void spaces between large particles until the addition of one more fine particle would result in two large particles losing contact. In the fines-percolated regime, the mechanical response is governed by fine grains. The percolation threshold of coarse material in the fine matrix is not well known. In the fourth regime (dilute suspension), coarse particles are not in contact with each other and have little effect on the material behavior.

The quantity of fines in a matrix, such that a small change in the mixture ratio would lead to a significant change in behavior, is known as the threshold fines content (f_c^{th}). For $f_c < f_c^{th}$, intergranular contact friction plays the primary role, while the coarse grains provide the strength of the structure. With the continued addition of further fines, the coarse grains become separated from each other and the coarse–coarse contacts dissipate. The mechanical behavior of the mixture is different beyond this threshold, as the fines begin to make a substantial contribution to its load-bearing force-chain network (Radjai et al. 1998), increasing the shear strength of the soil. At $f_c > f_c^{th}$, the coarse particles start to separate, producing a secondary reinforcing effect (Thevanayagam et al. 2002; Yang et al. 2015).

Yang et al. (2006a) noted that critical state lines in the $e - \log p'_{cr}$ space initially move downward with increasing fines content, until a certain amount of fines content leads to the lowest position, after which the critical-state line begins to move back upward with the addition of more fines. They defined the f_c^{th} as the fines content at which movement of the critical-state line in the

Table 2. Threshold fines contents of fines used in this study

Parameter	Equation	*WS*	*UC*	*DS*
f_c^{th} (%)	Eq. (5)	32	39	36
	Eq. (6)	28	28	15

$e - \log p'_{cr}$ space reversed. Therefore, it is necessary to approximate the threshold fines content before analyzing the behavior of a mixture. Rahman et al. (2008) presented an empirical equation to estimate the f_c^{th} or, as they noted, the point at which fine-in-coarse changes to coarse-in-fine packing

$$f_c^{th} = 40\left(\frac{1}{1+e^{\alpha-\beta\chi}} + \frac{1}{\chi}\right) \tag{5}$$

where $\alpha = 0.5$; $\beta = 0.13$; and $\chi = D_{10}/d_{50}$, where D_{10} and d_{50} = effective size of the sand and mean size of the fines, respectively. In using this equation, the specific gravity of the fines was assumed to be similar to that of the coarse grains. Hazirbaba (2005) and Choo and Burns (2014) considered the fines content by mass percentage, and obtained the following formula to calculate f_c^{th}:

$$f_c^{th} = \frac{W_{fines}}{W_{sand} + W_{fines}} = \frac{G_{sf} e_s}{G_{sf} e_s + G_{ss}(1 + e_f)} \tag{6}$$

where W_{fines} = fines solid weight; W_{sand} = sand solid weight; G_{sf} and G_{ss} = specific gravity of the fines and sand; and e_f and e_s = void ratio of the fines in the voids of the sand matrix and sand, respectively.

The computed f_c^{th} for the different fines is presented in Table 2. As can be seen, there is a considerable difference between the f_c^{th} approximated using Eqs. (5) and (6). These differences can be attributed to the different perspectives these equations were developed from. In Eq. (5), the size disparity ratio is the primary consideration, while Eq. (6) focuses on the origin of the mixture constituents. The advantage of Eq. (6) is that it uses the specific gravities for defining f_c^{th} and can account for the different origins of the sand and fines; consequently, it was used in this study to estimate f_c^{th}.

Equivalent Intergranular Void Ratio

As the amount of fines increases in a soil mixture, the fine particles begin to impede the coarse grain contacts (Zlatović and Ishihara 1995). That is, at high fines contents, some fine particles become positioned between the coarse particles, contributing to the load-bearing force chains of the coarse particles (Radjai et al. 1998). As the amount of fines is increased in a soil mixture, sand particle contacts begin to dissipate at the threshold fines content (Kuerbis et al. 1988; Pitman et al. 1994; Rahman 2011).

For $f_c < f_c^{th}$, fines remain in the voids between coarse grains as largely inactive particles that do not contribute to the soil's resistance. In order to take into account both the fines that simply occupy the void space and those that take part in the force-chain structure, Thevanayagam et al. (2002) suggested the equivalent intergranular void ratio (e^*). They also introduced a parameter, b, to represent the fraction of fine particles that touched and separated the coarse grains and participated actively in the force chains, which are considered to be part of the skeleton of the soil matrix

$$e^* = \frac{e + (1-b) f_c}{1 - (1-b) f_c} \tag{7}$$

where e = void ratio; f_c = fines content; and $b \in [0\ 1]$ = fraction of active fines. When $b = 0$, this means that none of the fines contribute to the soil skeleton, whereas $b = 1$ means that all of the fines actively take part in the soil skeleton. The effectiveness of parameter b has been thoroughly discussed by Thevanayagam (2000), Ni et al. (2004), and Yang et al. (2015). They observed a strong correlation between the mechanical behavior of mixtures and the equivalent intergranular void ratio.

Nonetheless, finding a physically reasonable value of b is complex, remaining the main challenge to using the equivalent intergranular void ratio among researchers. Several studies have assumed a constant value of b for a given sand–silt mix. Thevanayagam et al. (2003) suggested that b depended upon the uniformity coefficient of the coarse and fine materials and used $b = 0.35$ for an Ottawa sand–silt mixture. Ni et al. (2004) concluded that the value of b was a function of effective size and the mean size of the sand and fines, using $b = 0.25$ for a Toyoura sand–silt mixture. Yang et al. (2006b) used $b = 0.25$ for up to the threshold fines content and $b = 0.4$ at the threshold fines content. Kanagalingam and Thevanayagam (2005) and Ni et al. (2004) used a correlation between soil index properties to back-calculate the b value.

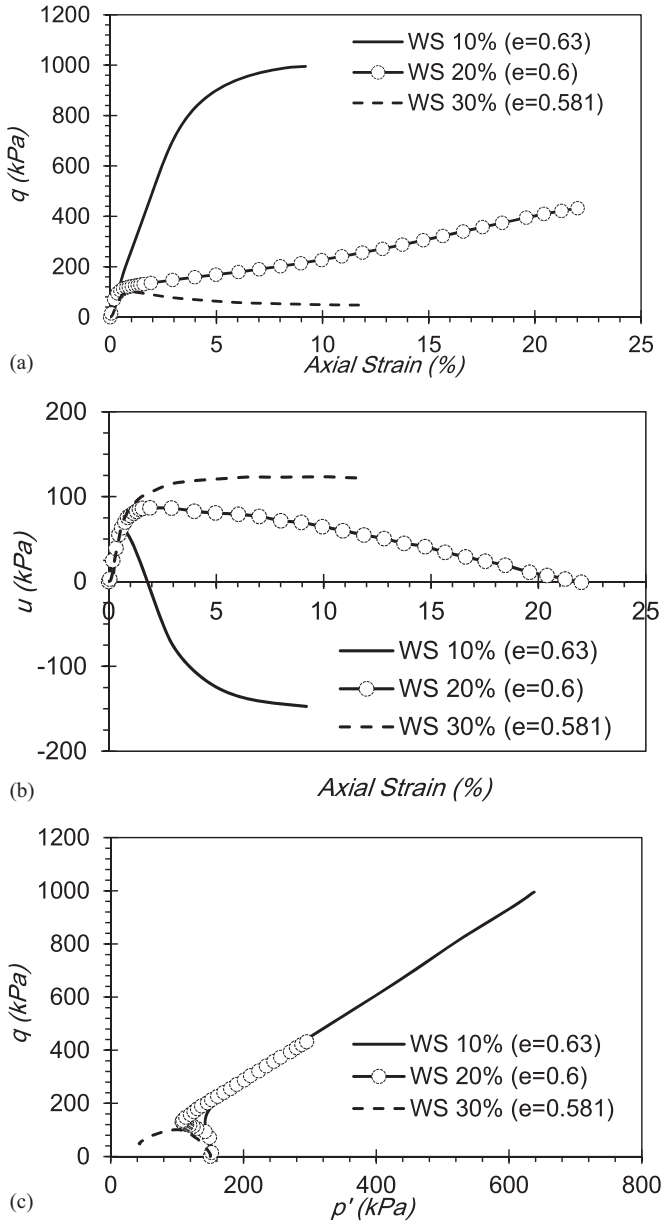

Fig. 6. (a) Deviatoric stress versus axial strain; (b) excess pore pressure versus axial strain; and (c) $q - p'$ data for some of the WS mixtures.

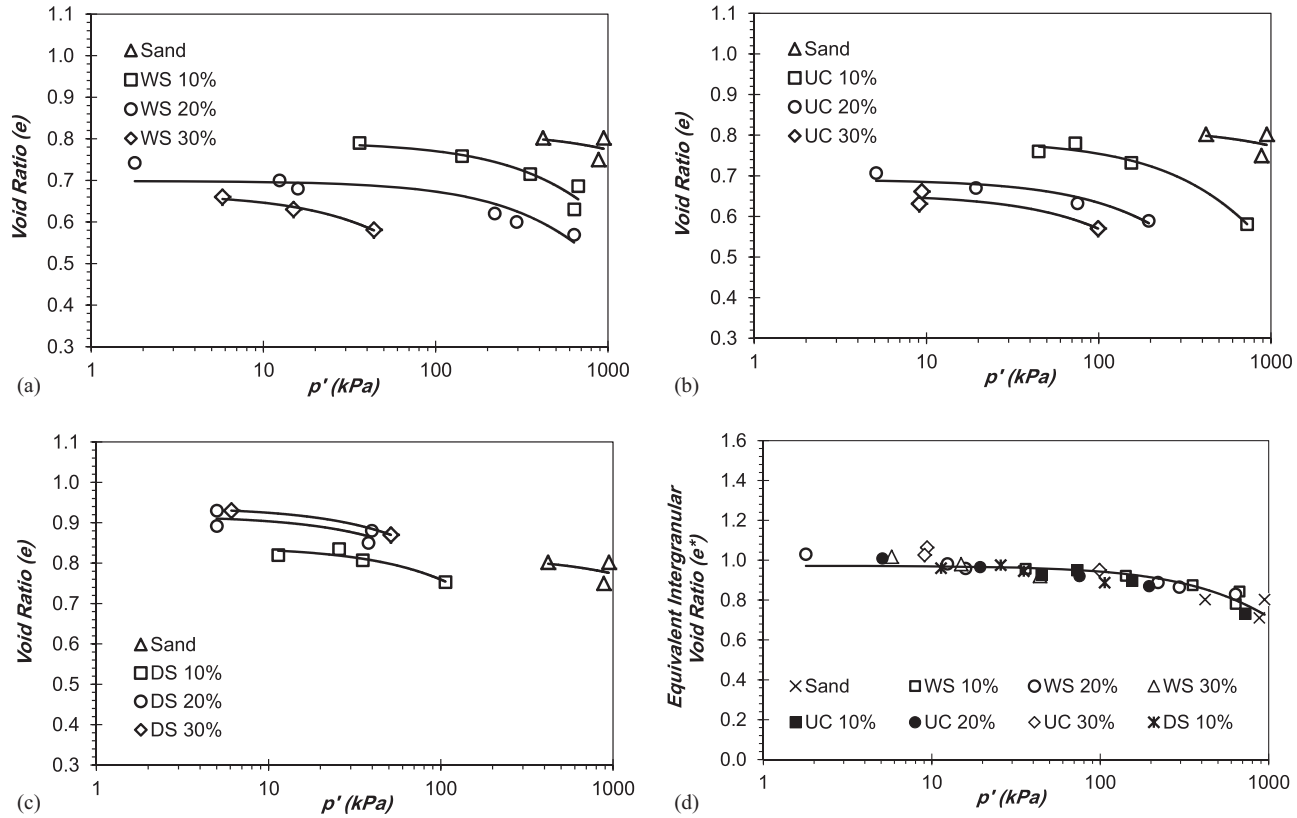

Fig. 7. Critical state loci of mixtures in the $e - \log p'_{cr}$ space for: (a) WS mixtures; (b) UC mixtures; (c) DS mixtures; and (d) $e^* - \log p'_{cr}$ for the mixtures, with the equivalent intergranular void ratio calculated using Eq. (7) with the threshold fines content from Eq. (6) and the "b" parameter from Eq. (8).

Rahman and Lo (2008) proposed the following empirical formula for b, based on a study by McGeary (1961) on binary packing and the factors affecting the amount of active fines (Lade et al. 1998):

$$b = \left\{1 - \exp\left(-0.3\frac{f_c/f_c^{th}}{1-(1/\chi)^{0.25}}\right)\right\}\left(\frac{1}{\chi}\frac{f_c}{f_c^{th}}\right)^{(1/\chi)} \quad (8)$$

where all the terms have been previously defined.

Mechanical Testing

Specimen Preparation

Sand–fines mixtures were prepared by mixing the host sand with the fines by mass percentage. Density-controlled moist tamping was applied. Specimens were prepared in 10 sublayers in a cylindrical mold with a diameter of 71 mm and a height of 142 mm. All the layers were constructed using the same weights of soil and compacted using a tamper to the desired density. An undercompaction procedure was used to improve the uniformity of the specimens (Ladd 1978; Naeini and Baziar 2004). Segregation in sand–fines mixtures is a common phenomenon during specimen preparation, but moist tamping minimizes the separation between the coarse and fine grains (Yang et al. 2006a).

Triaxial Compression Test

After mounting, the specimens were flushed with carbon dioxide for an hour, followed by flushing with de-aired water. During either the sample preparation or saturation process, the fines can potentially become mobilized. Two techniques were thus employed to avoid loss of the fines: placing wetted filter paper over porous stones during specimen preparation and percolating water into the specimen at a very low rate. In all cases, the B-value measured exceeded 0.96 prior to testing, and the samples were assumed to be saturated (Bouferra et al. 2007). The specimens were isotropically consolidated and sheared with the drainage valves closed. Fig. 6 represents the undrained monotonic behavior of the mixtures.

Results

Critical State Loci in e – log p'_{cr} Space

Fig. 7 shows the critical-state data from the test series in terms of void ratio versus the mean effective stress at the critical state, p'_{cr}. At the same void ratio, p'_{cr} decreased, and the critical state line (CSL) moved downward as the amount of fines increased in the WS and UC mixtures. This is consistent with observations from previous works (e.g., Zlatović and Ishihara 1995; Thevanayagam et al. 2002; Rahman et al. 2008; Yang et al. 2015; Ng et al. 2022). Mixtures prepared with the DS show the opposite behavior, increasing the fines content moved the CSL upward. Yang et al. (2015) pointed out that the CSL in the $e - \log p'_{cr}$ space was not necessarily a straight line and could be a curve. We noted that the curvature was not due to particle breakage because the stresses required for crushing silica sands is much higher than that experienced during the shearing (e.g., Verdugo and Ishihara 1996; Ghafghazi et al. 2014).

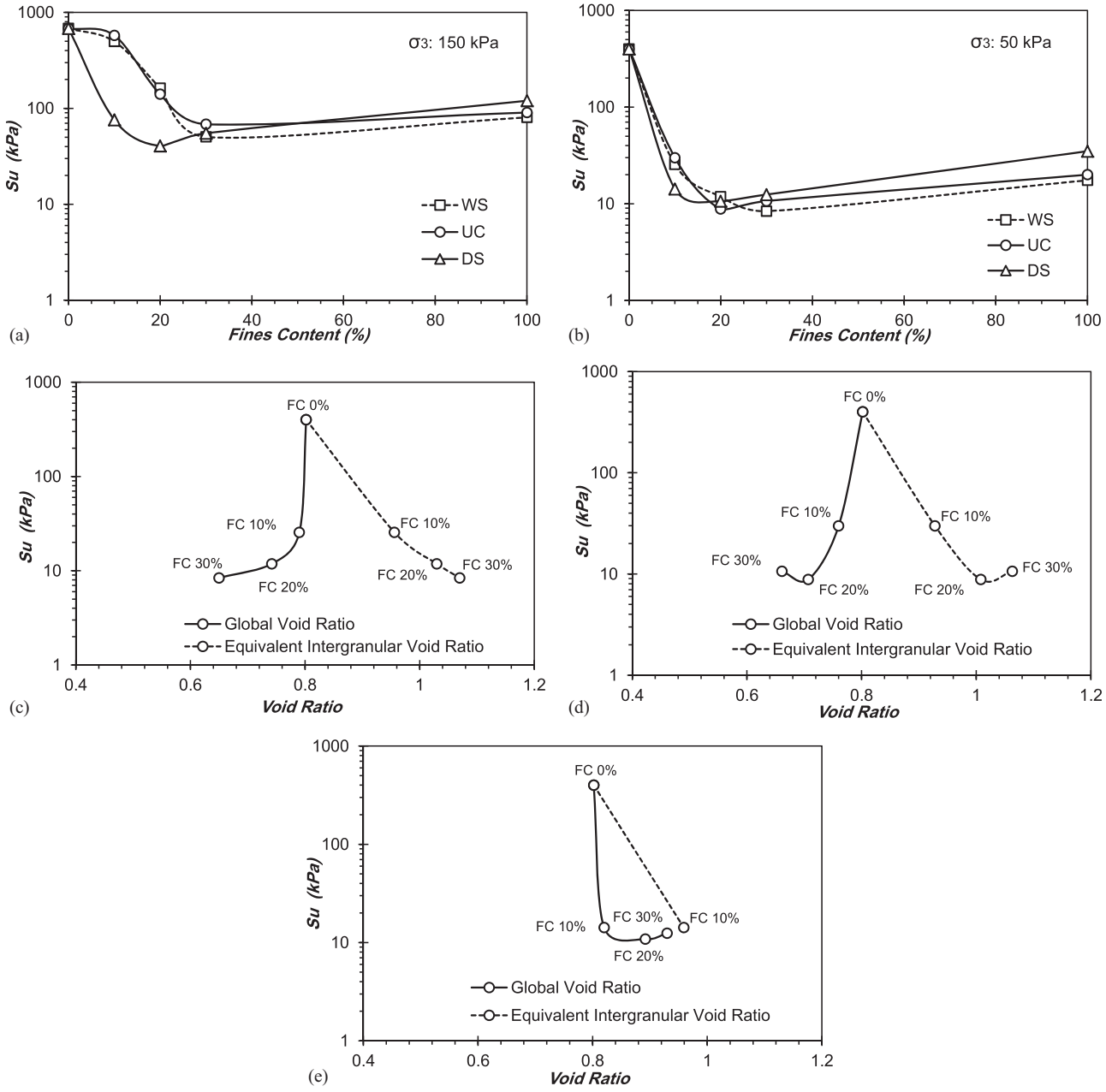

Fig. 8. Undrained shear strength of mixtures with different fines contents at confinements of (a) 150 kPa; and (b) 50 kPa. Undrained shear strength of mixtures at confinements of 50 kPa: (c) WS; (d) UC; and (e) DS.

Undrained Shear Strength

Fig. 8(a) shows the undrained shear strength response of mixtures with different types of fines as a function of the fines content. An obvious conclusion that could be drawn was that the undrained shear strength decreased dramatically with increasing fines content until f_c^{th}, then increased slightly to the undrained shear strength of pure, fine-grained soils. The DS mixtures with a 10% fines content had a greater loss of strength than the WS and US mixtures. In Figs. 8(c–e), the undrained shear strength is presented versus the void ratio, e, and the equivalent intergranular void ratio, e^*. These plots show that the global void ratio decreased with the addition of the fines in the WS, UC, and DS mixtures, while the undrained shear strength decreased appreciably. A common interpretation is that fines act as a lubricant, allowing the coarse grains to slide past one another more easily during shear, and thus leading to a loss in strength. In the equivalent intergranular framework, however, when $f_c < f_c^{th}$, the active fines particles contributed to the force-chain structure and caused the coarse particles to become separated. Thus, the intergranular friction between the coarse grains started to dissipate. It is clear that, at a given fines content, the intergranular void ratio was higher than the global void ratio [dashed lines in Figs. 8(c–e)].

Instability and Collapsibility

Onset of Flow Liquefaction

Instability has been recognized as one of the failure mechanisms that play a significant role in the performance of geotechnical

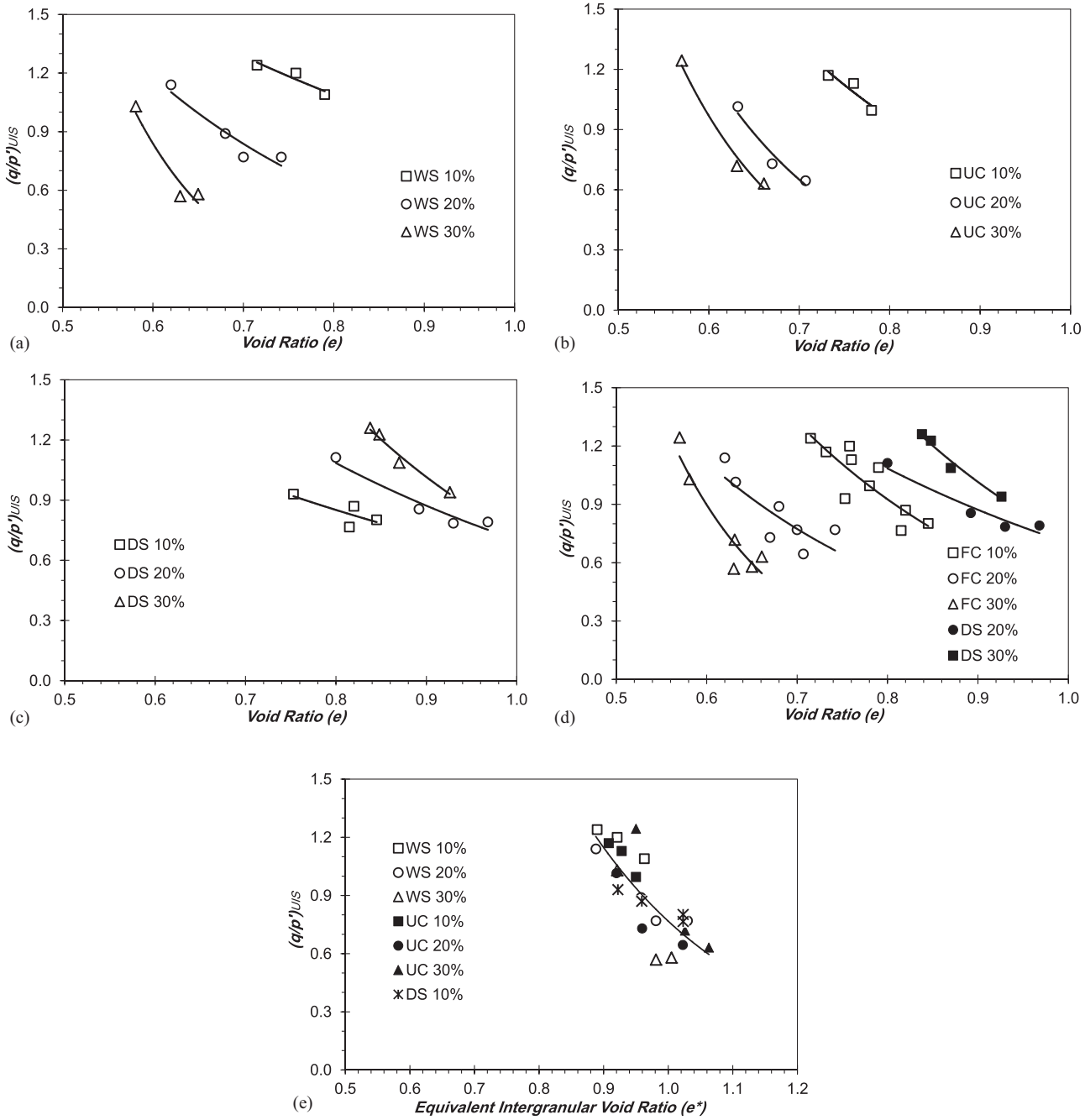

Fig. 9. Stress ratio of undrained instability: (a–d) versus void ratio; and (e) versus equivalent intergranular void ratio.

structures (Lade 1993; Leong and Chu 2002; Yang et al. 2006b). Some of the mixtures tested in this work exhibited a strength peak at small strain, followed by instability and runaway deformation. This plastic strain was a response of the soil attempting to support a given load. This phenomenon is recognized as flow liquefaction (Ishihara 1993; Yang 2002). The initiation of flow liquefaction and loss of strength can be characterized by the peak stress ratio in the undrained instability state, $(q/p')_{UIS}$ (Vaid and Chern 1985; Yang 2002). The peak stress ratio, as a function of the global void ratio, is presented in Fig. 9. No significant differences were observed between the WS and UC mixtures. However, at higher fines contents (20% and 30%) in the DS mixtures, appreciably higher void ratios were recorded than in the other mixtures, almost certainly due to the high intraparticle porosity of the diatomaceous grains.

Collapsibility Index

The collapsibility index (I_c) is used to quantify the loss of strength when strain-softening takes place, and the shear strength of soil reaches its lowest residual value (Bishop 1967; Yang and Wei 2012)

$$I_c = \frac{q_{UIS} - q_{min}}{q_{UIS}} \tag{9}$$

where q_{UIS} = deviatoric stress at the onset of instability; and q_{min} = residual deviatoric stress in the critical state or in the quasisteady state (QSS), when a QSS exists. It can be inferred from Eq. (9) that I_c indicates the degree of collapsibility at a value varying from 0 for a dilative response to 1 for complete liquefaction. Fig. 10 presents the values of the I_c for mixtures at 150 kPa

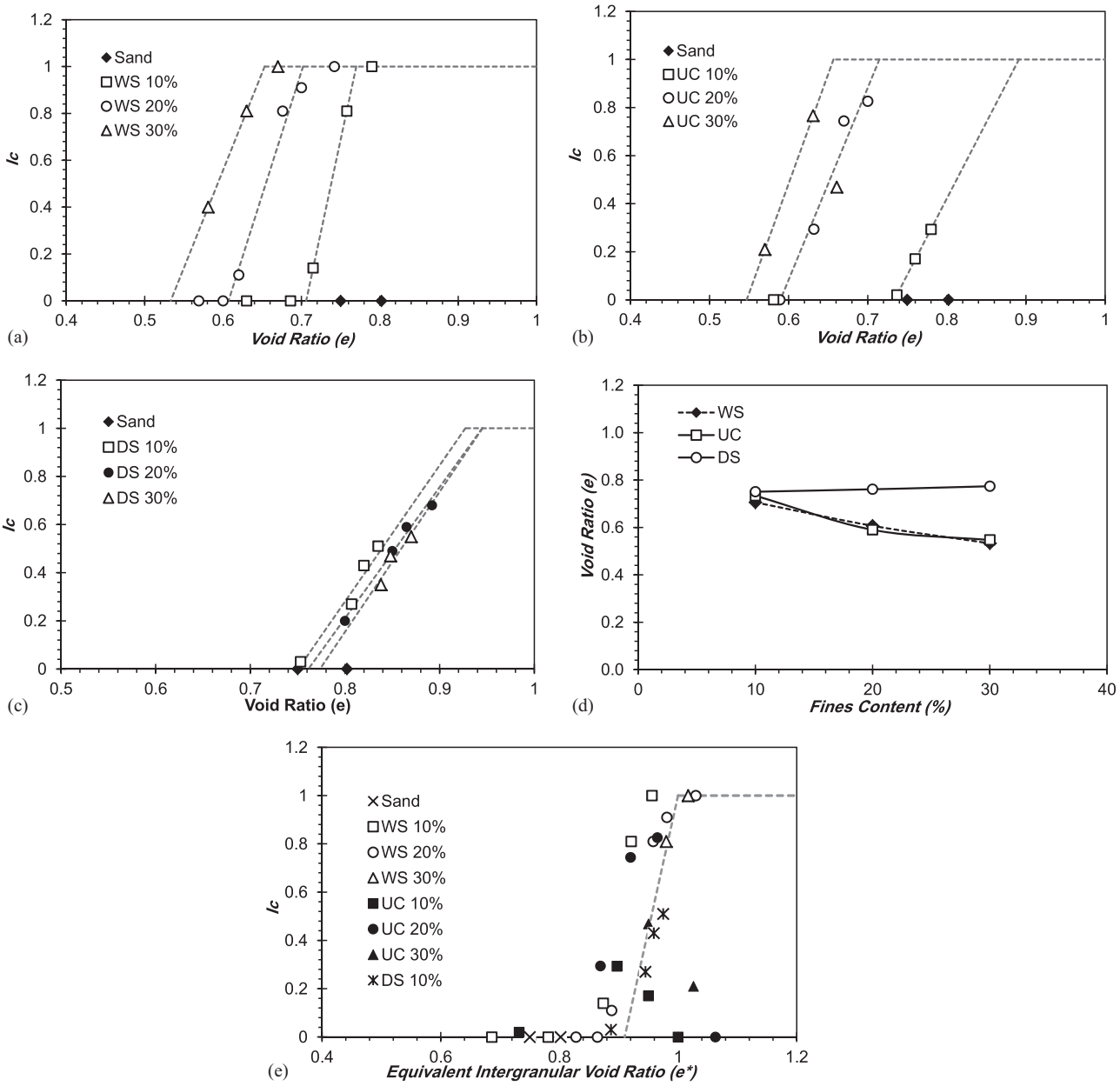

Fig. 10. Variation in collapsibility with (a–c) void ratio; and (d) triggering void ratio. (e) Collapsibility of mixtures versus equivalent intergranular void ratio.

confinement. The triggering void ratio, e_{tg}, and terminative void ratio, e_{tm}, are known to be the thresholds for the beginning of collapsibility and the onset of complete liquefaction, respectively (Yang and Wei 2012) [Fig. 10(d)].

Collapse Potential and Dilation Index

The collapse potential (*CP*) and resistance to further deformation (*RFD*) are two indices that quantify the tendency of mixtures to collapse and strain-harden, respectively (Thevanayagam et al. 2002). The *CP* was introduced as a maximum positive pore water pressure ratio that is generated during monotonic undrained loading

$$CP = \frac{\Delta u_{sh}}{\sigma_c'} \tag{10}$$

where Δu_{sh} = shear-induced excess pore water pressure; and σ_c' = effective confining stress. *CP* values vary from 0 for samples that have negative shear-induced pore water pressure from the beginning of the test to 1 for specimens that experience complete-flow liquefaction (Fig. 11).

The *RFD* index quantifies the strain-hardening tendency of mixtures by describing the degree of dilation beyond the point of maximum positive pore water pressure

$$RFD = \frac{p_{cr}' - p_{pt}'}{p_{cr}'} \tag{11}$$

where p_{cr}' and p_{pt}' = effective mean stress at the critical-state and phase transformation points, respectively. The maximum pore water pressure occurs at the phase-transformation point. Beyond this point, the specimen experiences dilative behavior. Figs. 11(c and d) illustrate the resistance of the mixture to large deformation.

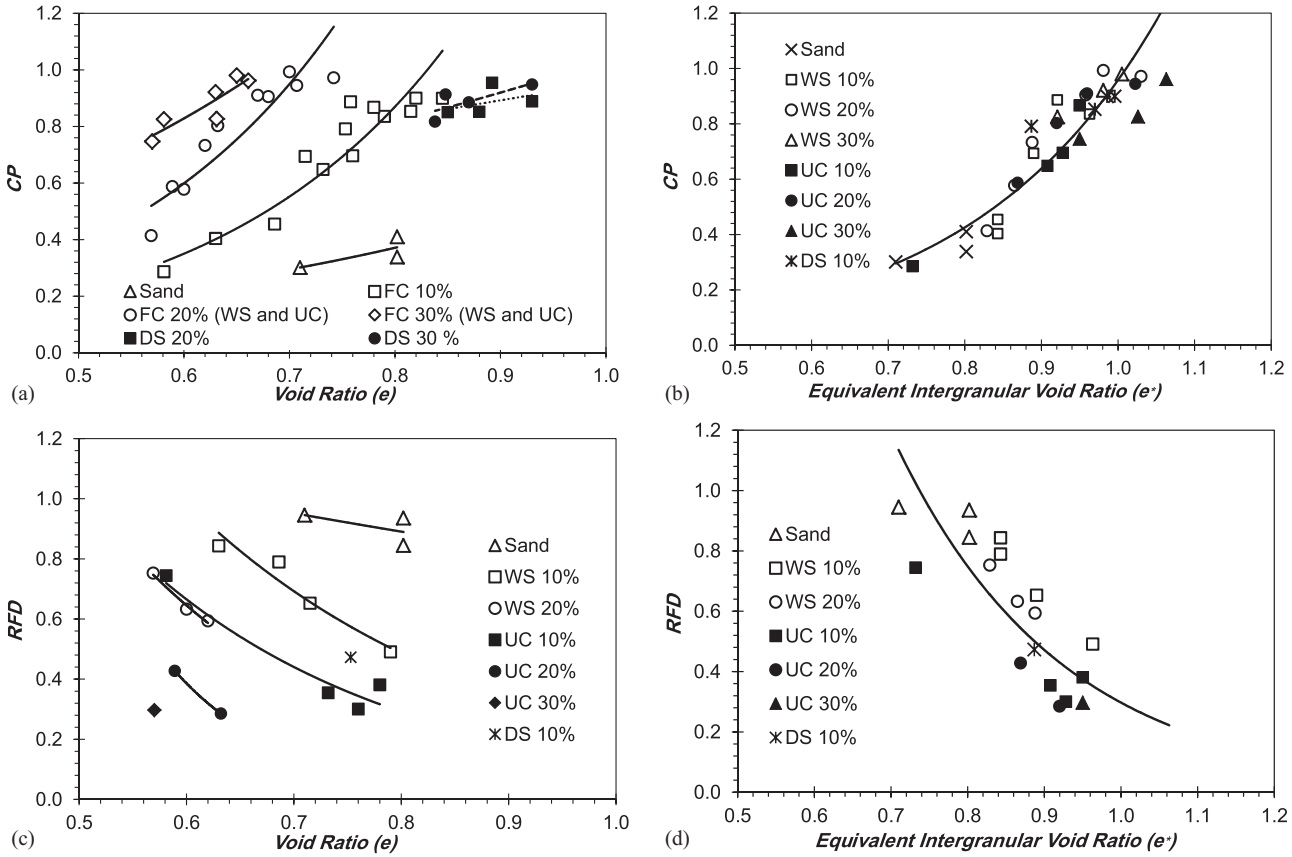

Fig. 11. (a and b) Variation in collapse potential with void ratio and equivalent intergranular void ratio. (c and d) Variation in *RFD* with void ratio and equivalent intergranular void ratio.

Discussion

Figs. 7(a–c) show that the CLSs in the $e - \log p'_{cr}$ space were dependent on the fines percentage and confirm that using the global void ratio as a state variable resulted in multiple CSLs. Fig. 7(c) indicates an upward movement in CSLs with increasing DS fines content that is contradictory to the behavior of the WS and UC mixtures. The threshold fines content for the DS mixtures was thus lower than for the other types of fines (Table 2), with fines contents of 20% and 30% being greater than f_c^{th}. Based on percolation theory, it is assumed that the critical-state behavior of mixtures with fines greater than f_c^{th} would be similar to that of pure fines. For $f_c < f_c^{th}$, the fine particles, to some degree, actively participated in the force-chain network and influenced the mechanical behavior of the coarse-grained–fines mixtures. The equivalent intergranular void ratio was introduced in order to take into account both the active fines and those that were simply occupying the void space. As presented in Table 2, the threshold fines content for the DS mixtures was 14%; therefore, the fines contents of 20% and 30% were greater than f_c^{th}. Hence, the data for the equivalent intergranular void ratio of the DS mixtures containing 20% and 30% fines are not shown. Fig. 7(d) presents the modified critical-state locus, in terms of the equivalent intergranular void ratio (e_{eq}). When the equivalent intergranular void ratio is used, the data collapse to a single critical state locus across all three types of fines.

Instability triggering was evaluated using the peak stress ratio $(q/p')_{UIS}$. In Fig. 9, the WS and US mixtures show stress-ratio curves as a function of the global downward void ratio shift (i.e., lower stress ratio) as the fines increased. This means instability was more likely for the WS and UC mixtures with higher fines contents. The DS mixtures demonstrated contrary behavior—by increasing the fines content in the DS mixtures from 10% to 30%, the $(q/p')_{UIS}$ curves shift upward (i.e., higher stress ratio), thus indicating less susceptibility to flow liquefaction. One conclusion that can be drawn from Fig. 9 is that the instability or flow liquefaction was triggered at lower stress ratios in the WS and UC mixtures than in the DS mixtures.

Fig. 10 shows the I_c. This index implicitly assigns a degree of collapsibility to the mixtures. The collapsibility lines in the WS and UC mixtures shifted toward the left as the fines content of the mixtures increased. For a given void ratio, the degree of collapsibility increased with increasing fines percentage, and the specimens became prone to collapse more easily than those with lower fines contents. Instability in the DS mixtures occurred at a higher void ratio. However, as the fines content increased, the specimens showed little reduction in their resistance to instability, followed by an enhancement in their resistance to progressive collapse. The specimen with a void ratio smaller than the triggering void ratio exhibited a dilative response ($I_c = 0$) to shearing, while above the triggering void ratio, contractive behavior dominated and instability commenced to varying degrees, resulting in strain-softening behavior. For void ratios greater than the terminative void ratio, e_{tm}, the response of the specimens would be flow liquefaction with no residual strength ($I_c = 1$).

The triggering void ratio depends on the nature of the fines and the amount of fines in the mixtures [Fig. 10(d)]. The DS mixtures were less prone to strain-softening behavior, and partial instability occurred at a higher void ratio compared with the WS and UC mixtures. A potential cause of this behavior might have been the interlocking of the diatom particles.

The *CP* and *RFD* indices were used to quantify the strain-softening and -hardening tendencies of the mixtures to shearing,

respectively. As indicated in Figs. 11(a and b), increasing the fines content led to an increase in shear-induced excess pore water pressure that could be the reason for instability being encountered much earlier in the specimen with a higher fines content. As can also be seen in Fig. 11(a), the DS mixtures exhibited contrary behaviors and, despite developing high pore water pressures, their increasing void ratios resulted in near-constant values of the *CP* index, implying a higher resistance to flow liquefaction. No significant difference was observed between the WS and UC mixtures containing the same percentage of fines.

The *RFD* index was taken as 0 for specimens exhibiting strain-softening behavior and 1 for specimens that dilated from the start of shearing. Figs. 11(c and d) show the *RFD* results for the specimens that dilated to some degree. For mixtures with the same amount of fines, the WS specimens showed a higher degree of dilation compared with the UC specimens. This finding is consistent with the understanding that plasticity inhibits dilation.

Despite the high nominal *PI* of the DS ($PI = 70$), its conventional electrical sensitivity was quite low. The behavioral conformity in terms of the intergranular void ratio of the DS mixtures with the WS and UC mixtures confirmed that the true plasticity (which arises from electrochemical forces) of the DS was low.

As shown in Figs. 9(e), 10(e), and 11(d), there are still some differences with the use of e^* that can be attributed to the effect of a variety of factors, such as particle shape, sand and fines size disparity, and the plasticity of the fines at different stages of shearing. Various experimental studies have explored the fraction of active fines using the large deformation behavior of granular mixtures, while the contribution of active fines in stress transmission through coarse-grained–fines packing at different shearing stages, such as the peak and phase-transformation points, remains an area of active research.

Conclusions

The instability of sand–fines mixtures is traditionally characterized using the global void ratio as a state variable. The existence of multiple CSLs in the $e - \log p'_{cr}$ space for different mixtures of the same material expresses the dependency of the CSLs to the fines content. We suggest the use of the equivalent intergranular void ratio as a state variable in order to resolve some inconsistencies in explaining the behavior of coarse-grained–fines mixtures, such as numerous CSLs and an increased susceptibility to instability with increasing fines content, despite a lower void ratio. Our results indicate that the equivalent intergranular void ratio can capture the influence of the fines, and provide a robust correlation with many aspects of the mechanical behavior of coarse-grained–fines mixtures. Additional observations include:

1. DS has a high PI, but low electrical sensitivity. This suggests that the reason for the high PI is a consequence of the porous structure of DS—which can hold water–and not the electrostatic forces that are responsible for high plasticity in clays;
2. Adding fines to sand leads to multiple CSLs in the $e - \log p'_{cr}$ space. The WS and US mixtures exhibited downward CSL movement, whereas the DS mixtures showed the opposite behavior, which was due to the lower f_c^{th} of the DS compared with the other types of fines. Both the 20% and 30% DS mixtures changed from fine-in-coarse to coarse-in-fine packing. Thus, the CSLs showed upward movement in the $e - \log p'_{cr}$ space;
3. Using the equivalent intergranular void ratio as a density state variable led to a single critical-state curve for mixtures with fines contents that were less than f_c^{th}, with all the data falling into a narrow band;
4. For a given global void ratio, the degree of collapsibility increased with increasing fines content in the WS and UC specimens, whereas the DS specimens did not show a substantial change in I_c while showing a higher triggering void ratio, e_{tg};
5. The strain-softening and -hardening behaviors were quantified using the *CP* and *RFD* indices, respectively. At a given global void ratio, and with and increasing fines content, the *CP* increased in the WS and UC specimens due to shear-induced positive pore water pressure; and
6. In mixtures with the same amount of fines, the WS specimens showed more of a tendency to strain-harden (higher degree of dilation) compared with the UC specimens, but no dilation behavior was observed in the DS mixtures.

Data Availability Statement

All data, models, or codes that support the findings of this study are available from the corresponding author upon reasonable request.

Acknowledgments

The work described in this manuscript was made possible through support from the Cascadia Lifelines Program (CLiP). EY and TME were partially supported by the U.S. National Science Foundation (CMMI-1933355) during portions of this work. This support is gratefully acknowledged.

References

Altun, S., A. B. Göktepe, and C. Akgüner. 2005. "Cyclic shear strength of silts and sands under cyclic loading." In Earthquake Engineering and Soil Dynamics, Geotechnical Special Publication 133, edited by R. W. Kalinski, S. L. Kramer, M. Manzari, and J. Pauschke, 1–11. Reston, VA: ASCE.

Amini, F., and G. Z. Qi. 2000. "Liquefaction testing of stratified silty sands." *J. Geotech. Geoenviron. Eng.* 126 (3): 208–217. https://doi.org/10.1061/(ASCE)1090-0241(2000)126:3(208).

ASTM. 2004. *Standard test methods for particle-size distribution (gradation) of soils using sieve analysis*. ASTM D6913. West Conshohocken, PA: ASTM.

ASTM. 2016. *Standard test method for particle-size distribution (gradation) of fine grained soils using the sedimentation (hydrometer) analysis*. ASTM D7928. West Conshohocken, PA: ASTM.

Belkhatir, M., H. Missoum, A. Arab, N. Della, and T. Schanz. 2011. "Undrained shear strength of sand-silt mixture: Effect of intergranular void ratio and other parameters." *KSCE J. Civ. Eng.* 15 (8): 1335–1342. https://doi.org/10.1007/s12205-011-1051-x.

Bishop, A. 1967. "Progressive failure–with special reference to the mechanism causing it." *Rock Mech. Rock Eng.* 2, 142–150. https://doi.org/10.1007/BF01079687.

Bolton Seed, H., K. Tokimatsu, L. F. Harder, and R. M. Chung. 1985. "Influence of SPT procedures in soil liquefaction resistance evaluations." *J. Geotech. Eng.* 111 (12): 1425–1445. https://doi.org/10.1061/(ASCE)0733-9410(1985)111:12(1425).

Bouckovalas, G. D., K. I. Andrianopoulos, and A. G. Papadimitriou. 2003. "A critical state interpretation for the cyclic liquefaction resistance of silty sands." *Soil Dyn. Earthquake Eng.* 23 (2): 115–125. https://doi.org/10.1016/S0267-7261(02)00156-2.

Bouferra, R., N. Benseddiq, and I. Shahrour. 2007. "Saturation and preloading effects on the cyclic behavior of sand." *Int. J. Geomech.* 7 (5): 396–401. https://doi.org/10.1061/(ASCE)1532-3641(2007)7:5(396).

Bouferra, R., and I. Shahrour. 2004. "Influence of fines on the resistance to liquefaction of a clayey sand." *Proc., Inst. Civ. Eng. – Ground Improv.* 8 (1): 1–5. https://doi.org/10.1680/grim.2004.8.1.1.
Caicedo, B., C. Mendoza, F. López, and A. Lizcano. 2018. "Behavior of diatomaceous soil in lacustrine deposits of Bogotá, Colombia." *J. Rock Mech. Geotech. Eng.* 10 (2): 367–379. https://doi.org/10.1016/j.jrmge.2017.10.005.
Casagrande, A. 1958. "Notes on the design of the liquid limit device." *Géotechnique* 8 (2): 84–91. https://doi.org/10.1680/geot.1958.8.2.84.
Chien, L.-K., Y.-N. Oh, and C.-H. Chang. 2002. "Effects of fines content on liquefaction strength and dynamic settlement of reclaimed soil." *Can. Geotech. J.* 39 (1): 254–265. https://doi.org/10.1139/t01-083.
Choo, H., and S. E. Burns. 2014. "Effect of overconsolidation ratio on dynamic properties of binary mixtures of silica particles." *Soil Dyn. Earthquake Eng.* 60: 44–50. https://doi.org/10.1016/j.soildyn.2014.01.015.
Evans, T. M., and D. Moug. 2020. "Diatomaceous soils: A less than cromulent engineering material." In *Geotechnics for sustainable infrastructure development*, edited by P. Duc Long and N. Dung, 709–716. Singapore: Springer.
Evans, T. M., and D. C. Simpson. 2015. "Innovative data acquisition for the fall cone test in teaching and research." *Geotech. Test. J.* 38 (3): 20140236. https://doi.org/10.1520/GTJ20140236.
Feng, T.-W. 2000. "Fall-cone penetration and water content relationship of clays." *Géotechnique* 50 (2): 181–187. https://doi.org/10.1680/geot.2000.50.2.181.
Feng, T.-W. 2001. "A linear log d log w model for the determination of consistency limits of soils." *Can. Geotech. J.* 38 (6): 1335–1342.
Furnas, C. C. 1928. *The relations between specific volume, voids, and size composition in systems of broken solids of mixed sizes*. Washington, DC: Dept. of Commerce, Bureau of Mines. Rep. of Investigations, 1–10.
Garga, V. K., and L. D. McKay. 1984. "Cyclic triaxial strength of mine tailings." *J. Geotech. Eng.* 110 (8): 1091–1105. https://doi.org/10.1061/(ASCE)0733-9410(1984)110:8(1091).
Ghafghazi, M., D. A. Shuttle, and J. T. DeJong. 2014. "Particle breakage and the critical state of sand." *Soils Found.* 54 (3): 451–461. https://doi.org/10.1016/j.sandf.2014.04.016.
Gobbi, S., M. P. Santisi d'Avila, L. Lenti, J.-F. Semblat, and P. Reiffsteck. 2022. "Effect of active plastic fine fraction on undrained behavior of binary granular mixtures." *Int. J. Geomech.* 22 (1): 06021035. https://doi.org/10.1061/(ASCE)GM.1943-5622.0002242.
Graton, L. C., and H. J. Fraser. 1935. "Systematic packing of spheres: With particular relation to porosity and permeability." *J. Geol.* 43(8, Part 1): 785–909. https://doi.org/10.1086/624386.
Guo, T., and S. Prakash. 1999. "Liquefaction of silts and silt-clay mixtures." *J. Geotech. Geoenviron. Eng.* 125 (8): 706–710. https://doi.org/10.1061/(ASCE)1090-0241(1999)125:8(706).
Hansbo, S. 1957. *A new approach to the determination of the shear strength of clay by the fall-cone test*. Stockholm, Sweden: Royal Swedish Geotechnical Institute.
Hazirbaba, K. 2005. "Pore pressure generation characteristics of sands and silty sands: A strain approach." Ph.D. thesis, Civil, Architectural, and Environmental Engineering, Univ. of Texas.
Hazirbaba, K., and E. M. Rathje. 2009. "Pore pressure generation of silty sands due to induced cyclic shear strains." *J. Geotech. Geoenviron. Eng.* 135 (12): 1892–1905. https://doi.org/10.1061/(ASCE)GT.1943-5606.0000147.
Herega, A. 2015. "Some applications of the percolation theory: Review of the century beginning." *J. Mater. Sci. Eng. A* 5 (12): 409–414. https://doi.org/10.17265/2161-6213/2015.11-12.004.
Ishihara, K. 1993. "Liquefaction and flow failure during earthquakes." *Géotechnique* 43 (3): 351–451. https://doi.org/10.1680/geot.1993.43.3.351.
Ishihara, K., M. Sodekawa, and Y. Tanaka. 1978. *Effects of overconsolidation on liquefaction characteristics of sands containing fines*. Dynamic Geotechnical Testing. West Conshohocken, PA: ASTM.
Ishihara, K., J. Troncoso, Y. Kawase, and Y. Takahashi. 1980. "Cyclic strength characteristics of tailings materials." *Soils Found.* 20 (4): 127–142. https://doi.org/10.3208/sandf1972.20.4_127.
Jang, J., and J. C. Santamarina. 2016. "Fines classification based on sensitivity to pore-fluid chemistry." *J. Geotech. Geoenviron. Eng.* 142 (4): 06015018. https://doi.org/10.1061/(ASCE)GT.1943-5606.0001420.
Kanagalingam, T., and S. Thevanayagam. 2005. "Discussion: Contribution of fines to the compressive strength of mixed soils." *Géotechnique* 55 (8): 627–628. https://doi.org/10.1680/geot.2005.55.8.627.
Khoubani, A., and T. M. Evans. 2017. "Discussion of "fines classification based on sensitivity to pore-fluid chemistry" by Junbong Jang and J. Carlos Santamarina." *J. Geotech. Geoenviron. Eng.* 143 (7): 07017008.
Khoubani, A., T. M. Evans, and T. S. Yun. 2020. "Thermal percolation in mixtures of monodisperse spheres." *Granular Matter* 22 (3): 60. https://doi.org/10.1007/s10035-020-01028-8.
Koester, J. P. 2018. "Triggering and post-liquefaction strength issues in fine-grained soils." In *Physics and mechanics of soil liquefaction*, edited by P. V. Lade and J. A. Yamamuro, 79–89. London: Routledge.
Koumoto, T., and G. T. Houlsby. 2001. "Theory and practice of the fall cone test." *Géotechnique* 51 (8): 701–712. https://doi.org/10.1680/geot.2001.51.8.701.
Kuerbis, R., D. Negussey, and Y. P. Vaid. 1988. "Effect of gradation and fines content on the undrained response of sand." *Geotech. Spec. Publ.* 21: 330–345.
Ladd, R. S. 1978. "Preparing test specimens using undercompaction." *Geotech. Test. J.* 1 (1): 16–23. https://doi.org/10.1520/GTJ10364J.
Lade, P. V. 1993. "Initiation of static instability in the submarine Nerlerk berm." *Can. Geotech. J.* 30 (6): 895–904. https://doi.org/10.1139/t93-088.
Lade, P. V., C. D. Liggio, and J. A. Yamamuro. 1998. "Effects of nonplastic fines on minimum and maximum void ratios of sand." *Geotech. Test. J.* 21 (4): 336–347. https://doi.org/10.1520/GTJ11373J.
Leong, W. K., and J. Chu. 2002. "Effect of undrained creep on instability behaviour of loose sand." *Can. Geotech. J.* 39 (6): 1399–1405. https://doi.org/10.1139/t02-076.
McGeary, R. K. 1961. "Mechanical packing of spherical particles." *J. Am. Ceram. Soc.* 44 (10): 513–522. https://doi.org/10.1111/j.1151-2916.1961.tb13716.x.
Mitchell, J. K., and K. Soga. 2005. Vol. 3 of *Fundamentals of soil behavior*. New York: Wiley.
Naeini, S. A., and M. H. Baziar. 2004. "Effect of fines content on steady-state strength of mixed and layered samples of a sand." *Soil Dyn. Earthquake Eng.* 24 (3): 181–187. https://doi.org/10.1016/j.soildyn.2003.11.003.
Ng, T.-T., W. Zhou, and G. Ma. 2022. "Numerical study of a binary mixture of similar ellipsoids of various particle shapes and fines contents." *Int. J. Geomech.* 22 (4): 04022022. https://doi.org/10.1061/(ASCE)GM.1943-5622.0002325.
Ni, Q., T. S. Tan, G. R. Dasari, and D. W. Hight. 2004. "Contribution of fines to the compressive strength of mixed soils." *Géotechnique* 54 (9): 561–569. https://doi.org/10.1680/geot.2004.54.9.561.
Okusa, S., S. Anma, and H. Maikuma. 1980. "Liquefaction of mine tailings in the 1978 Izu-Ohshima-Kinkai earthquake, central Japan." In *Proc., 7th World Conf. on Earthquake Engineering*, 8–13. Istanbul, Turkey: Turkish National Committee on Earthquake Engineering.
Park, S.-S., and Y.-S. Kim. 2013. "Liquefaction resistance of sands containing plastic fines with different plasticity." *J. Geotech. Geoenviron. Eng.* 139 (5): 825–830. https://doi.org/10.1061/(ASCE)GT.1943-5606.0000806.
Perlea, V. G. 2000. "Liquefaction of cohesive soils." In *Soil dynamics and liquefaction*, edited by R. Y. S. Pak, and J. Yamamura, *Geotechnical Special Publication* 107, 58–76. Reston, VA: ASCE.
Peters, J. F., and E. S. Berney. 2010. "Percolation threshold of sand-clay binary mixtures." *J. Geotech. Geoenviron. Eng.* 136 (2): 310–318. https://doi.org/10.1061/(ASCE)GT.1943-5606.0000211.
Pitman, T. D., P. K. Robertson, and D. C. Sego. 1994. "Influence of fines on the collapse of loose sands." *Can. Geotech. J.* 31 (5): 728–739. https://doi.org/10.1139/t94-084.
Polito, C. P., and J. R. Martin. 2001. "Effects of nonplastic fines on the liquefaction resistance of sands." *J. Geotech. Geoenviron. Eng.* 127 (5): 408–415. https://doi.org/10.1061/(ASCE)1090-0241(2001)127:5(408).
Porcino, D. D., and V. Diano. 2017. "The influence of non-plastic fines on pore water pressure generation and undrained shear strength of sand-silt mixtures." *Soil Dyn. Earthquake Eng.* 101: 311–321. https://doi.org/10.1016/j.soildyn.2017.07.015.
Radjai, F., D. E. Wolf, M. Jean, and J.-J. Moreau. 1998. "Bimodal character of stress transmission in granular packings." *Phys. Rev. Lett.* 80 (1): 61–64. https://doi.org/10.1103/PhysRevLett.80.61.

Rahman, M. M. 2011. "Comment on: "Influence of inter-granular void ratio on monotonic and cyclic undrained shear response of sandy soils" by M. Belkhatir, A. Arab, H. Missoum, T. Schanz [C. R. Mecanique 338 (2010) 290–303]." *C. R. Méc.* 339 (1): 58–62. https://doi.org/10.1016/j.crme.2010.12.009.

Rahman, M. M., and S. R. Lo. 2008. "The prediction of equivalent granular steady state line of loose sand with fines." *Geomech. Geoeng.* 3 (3): 179–190. https://doi.org/10.1080/17486020802206867.

Rahman, M. M., S. R. Lo, and C. T. Gnanendran. 2008. "On equivalent granular void ratio and steady state behaviour of loose sand with fines." *Can. Geotech. J.* 45 (10): 1439–1456. https://doi.org/10.1139/T08-064.

Rahman, M. M., and T. G. Sitharam. 2020. "Cyclic liquefaction screening of sand with non-plastic fines: Critical state approach." *Geosci. Front.* 11 (2): 429–438. https://doi.org/10.1016/j.gsf.2018.09.009.

Russell, E. R., and J. L. Mickle. 1970. "Liquid limit values by soil moisture tension." *J. Soil Mech. Found. Div.* 96 (3): 967–989. https://doi.org/10.1061/JSFEAQ.0001428.

Shen, C. K., J. L. Vrymoed, and C. K. Uyeno. 1977. "The effect of fines on liquefaction of sands." In Vol. 2 of *Proc., 9th ICSMFE*, 381–385. Tokyo, Japan: ICSMFE.

Sherwood, P. T., and M. D. Ryley. 1970. "An investigation of a cone-penetrometer method for the determination of the liquid limit." *Géotechnique* 20 (2): 203–208. https://doi.org/10.1680/geot.1970.20.2.203.

Simpson, D. C., and T. M. Evans. 2016. "Behavioral thresholds in mixtures of sand and kaolinite clay." *J. Geotech. Geoenviron. Eng.* 142 (2): 04015073. https://doi.org/10.1061/(ASCE)GT.1943-5606.0001391.

Skemption, A. W., and R. D. Northey. 1952. "The sensitivity of clays." *Géotechnique* 3 (1): 30–53. https://doi.org/10.1680/geot.1952.3.1.30.

Sonyok, D. R. 2015. *Effect of diatoms on index properties, compressibility, suction, and stiffness of diatomite-kaolin mixtures*. Las Cruces, NM: New Mexico State Univ.

Sowers, G., A. Vesić, and M. Grandolfi. 1960. "Penetration tests for liquid limit." In *Papers on Soils 1959 Meetings, Committe D-18*, 216–226. West Conshohocken, PA: ASTM International.

Thevanayagam, S. 2000. "Liquefaction potential and undrained fragility of silty soils." In *Proc., 12th World Conf. Earthquake Engineering*. Wellington, New Zealand: New Zealand Society of Earthquake Engineering.

Thevanayagam, S., T. Shenthan, and T. Kanagalingam. 2003. *Role of inter-granular contacts on mechanisms causing liquefaction & slope failures in silty sands*. Buffalo, NY: Univ. at Buffalo, State Univ. of New York, Dept. of Civil, Structural and Environmental Engineering.

Thevanayagam, S., T. Shenthan, S. Mohan, and J. Liang. 2002. "Undrained fragility of clean sands, silty sands, and sandy silts." *J. Geotech. Geoenviron. Eng.* 128 (10): 849–859. https://doi.org/10.1061/(ASCE)1090-0241(2002)128:10(849).

Throncoso, J. H., and R. Verdugo. 1985. "Silt content and dynamic behavior of tailing sands." *Int. Conf. Soil Mech. Found. Eng.* 11: 1311–1314.

Vaid, Y. P. 1994. "Liquefaction of silty soils. Ground failure under seismic condition." *Geotech. Spec. Publ.* 44: 1–16.

Vaid, Y. P., and J. C. Chern. 1985. "Cyclic and monotonic undrained response of saturated sands." In *Advances in the art of testing soils under cyclic conditions*, edited by V. Khosi, 120–147. Reston, VA: ASCE.

Verdugo, R., and K. Ishihara. 1996. "The steady state of sandy soils." *Soils Found.* 36 (2): 81–91. https://doi.org/10.3208/sandf.36.2_81.

Wang, J., E. Yazdani, and T. M. Evans. 2021. "Case study of a driven pile foundation in diatomaceous soil. I: Site characterization and engineering properties." *J. Rock Mech. Geotech. Eng.* 13 (2): 431–445. https://doi.org/10.1016/j.jrmge.2020.10.006.

White, H. E., and S. F. Walton. 1937. "Particle packing and particle shape." *J. Am. Ceram. Soc.* 20 (1–12): 155–166. https://doi.org/10.1111/j.1151-2916.1937.tb19882.x.

Wroth, C. P., and D. M. Wood. 1978. "The correlation of index properties with some basic engineering properties of soils." *Can. Geotech. J.* 15 (2): 137–145. https://doi.org/10.1139/t78-014.

Xenaki, V. C., and G. A. Athanasopoulos. 2003. "Liquefaction resistance of sand–silt mixtures: An experimental investigation of the effect of fines." *Soil Dyn. Earthquake Eng.* 23 (3): 1–12. https://doi.org/10.1016/S0267-7261(02)00210-5.

Yang, J. 2002. "Non-uniqueness of flow liquefaction line for loose sand." *Géotechnique* 52 (10): 757–760. https://doi.org/10.1680/geot.2002.52.10.757.

Yang, J., and L. M. Wei. 2012. "Collapse of loose sand with the addition of fines: The role of particle shape." *Géotechnique* 62 (12): 1111–1125. https://doi.org/10.1680/geot.11.P.062.

Yang, J., L. M. Wei, and B. B. Dai. 2015. "State variables for silty sands: Global void ratio or skeleton void ratio?" *Soils Found.* 55 (1): 99–111. https://doi.org/10.1016/j.sandf.2014.12.008.

Yang, S., S. Lacasse, and R. Sandven. 2006a. "Determination of the transitional fines content of mixtures of sand and non-plastic fines." *Geotech. Test. J.* 29 (2): 102–107.

Yang, S. L., R. Sandven, and L. Grande. 2006b. "Instability of sand–silt mixtures." *Soil Dyn. Earthquake Eng.* 26 (2–4): 183–190. https://doi.org/10.1016/j.soildyn.2004.11.027.

Yasuda, S., K. Wakamatsu, and H. Nagase. 1994. "Liquefaction of artificially filled silty sands." In Vol. 44 of *Ground Failures Under Seismic Conditions*, Geotech*nical* Special Publication, 91–104. New York: American Society of Civil Engineers.

Yazdani, E., J. Wang, and T. M. Evans. 2021. "Case study of a driven pile foundation in diatomaceous soil. II: Pile installation, dynamic analysis, and pore pressure generation." *J. Rock Mech. Geotech. Eng.* 13 (3): 11. https://doi.org/10.1016/j.jrmge.2020.10.005.

Zlatović, S., and K. Ishihara. 1995. "On the influence of nonplastic fines on residual strength." In Vol. 95 of *Proc., 1st Int. Conf. on Earthquake Geotechnical Engineering*, 239–244. Rotterdam, The Netherlands: A.A. Balkema.